

# Angular-dependent polarization-based plasmon light scattering for bioaffinity sensing

Kadir Aslan

*Institute of Fluorescence, Laboratory for Advanced Medical Plasmonics, Medical Biotechnology Center, University of Maryland Biotechnology Institute, 725 West Lombard Street, Baltimore, Maryland 21201*

Joseph R. Lakowicz

*Center for Fluorescence Spectroscopy, Medical Biotechnology Center, University of Maryland School of Medicine, 725 West Lombard Street, Baltimore, Maryland 21201*

Chris D. Geddes<sup>a)</sup>

*Institute of Fluorescence, Laboratory for Advanced Medical Plasmonics, Medical Biotechnology Center, University of Maryland Biotechnology Institute, 725 West Lombard Street, Baltimore, Maryland 21201 and Center for Fluorescence Spectroscopy, Medical Biotechnology Center, University of Maryland School of Medicine, 725 West Lombard Street, Baltimore, Maryland 21201*

(Received 29 July 2005; accepted 19 October 2005; published online 1 December 2005)

We describe an approach to affinity biosensing based on the depolarization of plasmon scatter of biotinylated-bovine serum albumin coated 20 nm gold colloids crosslinked by streptavidin. Our model system employs nanoparticles which initially scatter incident light with  $P \approx 1$ , in a Rayleigh-like manner. However, upon aggregation, the nanoparticles show a decreased polarization and an increased forward scatter, consistent with both plasmon near-field coupling and Mie like scatter, enabling large changes in polarization detectable at angles approaching  $180^\circ$ . © 2005 American Institute of Physics. [DOI: 10.1063/1.2137465]

The localized plasmon resonance of noble metal nanoparticles has led to the development of many sensors with unique properties in the last decade.<sup>1,2</sup> These nanoparticles exhibit strong UV-visible absorption bands that are not present in the bulk metal,<sup>1</sup> and which can lead to the brilliant colors observed for nanoparticles in solution, a function of both their absorption and scattering properties.<sup>1,2</sup>

The majority of sensors based on the nanoparticle surface plasmon resonance have been solution based,<sup>1</sup> where the sensitivity of the sensors is typically determined by the sensitivity of the surface plasmons themselves to interparticle coupling. When many particles, all supporting a surface plasmon resonance, are in close proximity, then they are able to interact electromagnetically through a dipole-dipole coupling mechanism.<sup>1,2</sup> This mechanism, which can occur up to two and half times the diameter of the particles,<sup>3</sup> broadens and redshifts the plasmon resonance bands, where smaller clusters of particles have similar plasmon resonance properties as compared to that of a larger single particle.<sup>1</sup> This has primarily lead to two main solution sensing formats using the nanoparticles, namely absorption/colorimetrically based,<sup>1,2</sup> and those which look for changes in plasmon light scattering properties.<sup>1,2</sup> While biosensing using plasmonic scatter is inherently a much more powerful technique, it is considerably less published.<sup>4-6</sup> We note a recently published method of wavelength-ratiometric plasmonic light scattering for glucose sensing by our laboratories.<sup>6</sup> Intuitively, these properties can be considered as a function of the nanoparticle's cross section,  $C_{\text{ext}}$ , which is comprised of both absorption,  $C_{\text{abs}}$ , and scattering,  $C_{\text{sca}}$ , components, where

$$C_{\text{ext}} = C_{\text{sca}} + C_{\text{abs}} \quad (1)$$

In addition to these two properties of nanoparticles, several other properties are known, but have been ill explored for biosensing. These include the spatial distribution of scatter and its subsequent polarization dependence. In this regard we have recently published an angular-ratiometric plasmon light scatter sensing platform,<sup>7</sup> based on the disruption of the  $\cos^2 \theta$  dependence of Rayleigh scatter, with excitation parallel to the scattering plane.<sup>7</sup> In this letter, we utilize plasmon light scattering to develop the concept of angular-dependent polarization-based plasmon light scattering for bioaffinity sensing. Here, the excitation is perpendicular to the scattering plane and so no  $\cos^2 \theta$  angular dependence of scatter is evident while the particles remain in the Rayleigh limit, i.e., diameter  $< 1/20\lambda$ . Subsequently, small Rayleigh like particles,<sup>8,9</sup> with an initial polarization approaching unity, aggregate together via a bioaffinity reaction. The induced aggregation changes the spatial distribution of polarized scatter around the sample. However, to maximize the observed signal and therefore downstream the sensitivity of the assay, we have selected particles which initially scatter light in a Rayleigh dependence. Upon aggregation, an increased forward scatter is observed (particles now scattering in the Mie limit),<sup>8-10</sup> enabling large changes in polarization to be subsequently observed at angles approaching  $180^\circ$ , the angle of forward scatter.

The change in polarization of light due to scattering has been known for many years, as first described by Rayleigh.<sup>11</sup> For the case where the incident light is polarized perpendicular to the scattering plane, then the extent of polarization,  $P$ , at any angle  $\theta$  is given by the expression

$$P = \frac{I_{\text{PERP}} - I_{\text{PAR}}}{I_{\text{PERP}} + I_{\text{PAR}}} \quad (2)$$

where  $I_{\text{PERP}}$  and  $I_{\text{PAR}}$  are the scattered intensities in the perpendicular and parallel planes respectively.  $P$  can be positive

<sup>a)</sup>Electronic mail: geddes@umbi.umd.edu



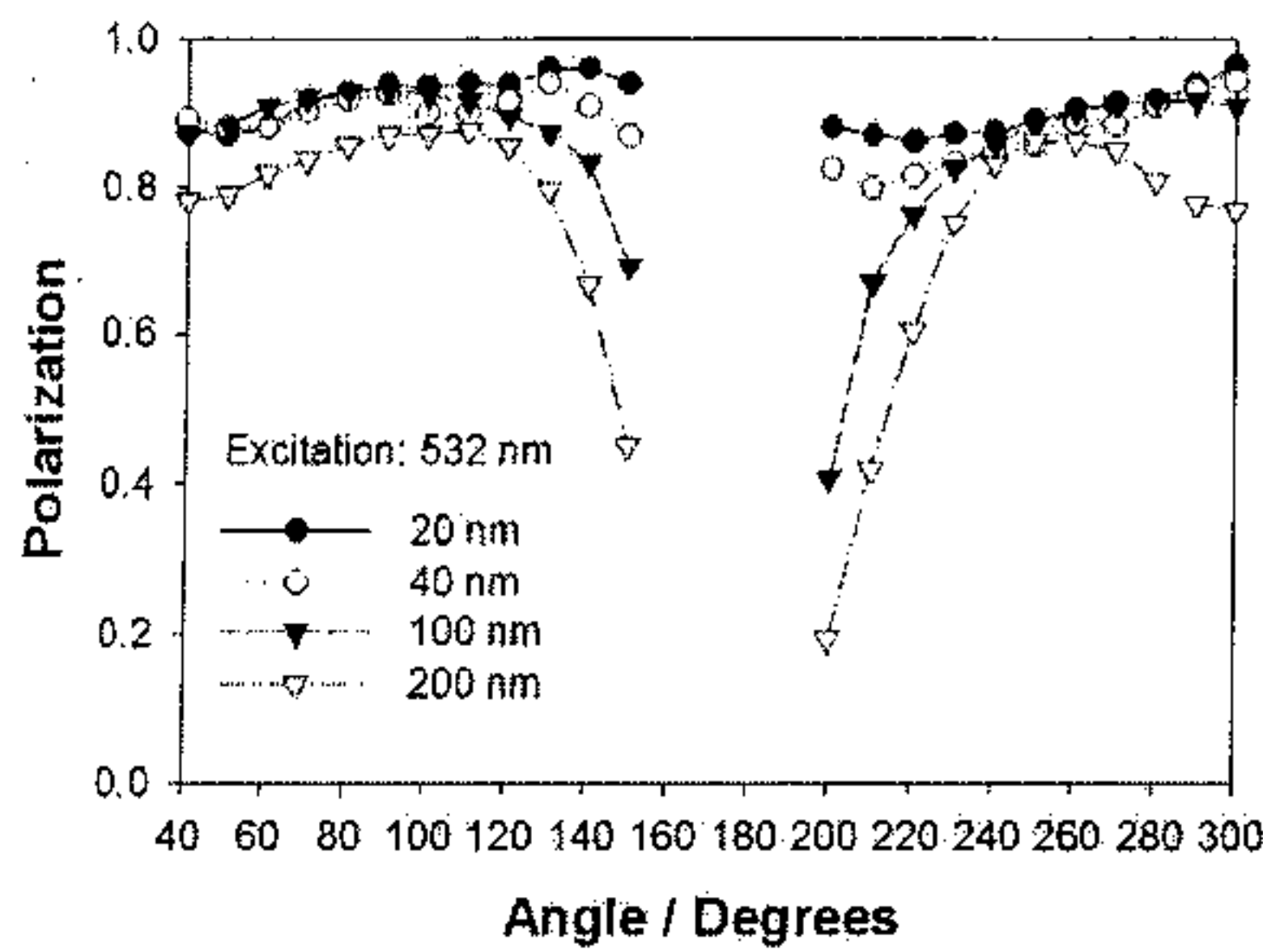


FIG. 1. Angular dependent-polarized scatter from different sized gold colloids.

or negative and  $|P| \leq 1$ .<sup>8,9</sup> For plane polarized light, the plasmon scattered light by a homogeneously sized and dilute solution approaches 1.<sup>8,9</sup> For light vertically polarized and perpendicular to the scattering plane, then the intensity of scatter is given by the well-known form of the Rayleigh expression

$$I_{\text{scatt}} = \frac{16\pi^4 a^6 n_{\text{med}}^4 I_0}{r^2 \lambda^4} \left| \frac{m^2 - 1}{m^2 + 2} \right|^2, \quad (3)$$

where  $I_0$  is the incident intensity of monochromatic light,  $n_{\text{med}}$  is the refractive index surrounding the particle,  $m$  is the refractive index of the bulk particle material, and  $r$  is the distance between the particle and where the scattered light is detected. Here, there is no angular dependence of scatter. In the case where the excitation polarization is parallel to the scattering plane, then the scattering intensity for small homogeneous spherical particle with radius  $a$ , that is much smaller than the wavelength,  $\lambda$ , of the incident beam, is given by a slightly different form of the Rayleigh expression<sup>8,9,11</sup>

$$I_{\text{scatt}} = \frac{16\pi^4 a^6 n_{\text{med}}^4 I_0}{r^2 \lambda^4} \left| \frac{m^2 - 1}{m^2 + 2} \right|^2 \cos^2 \theta. \quad (4)$$

In this condition, a  $\cos^2 \theta$  angular dependence of scatter is observed in the scattering plane. The intensity is highest at the observation angles  $0^\circ$  and  $180^\circ$  and minimum at  $90^\circ$  and  $270^\circ$  and is proportional to  $\cos^2 \theta$  at all other angles. In this letter, we employ excitation polarization perpendicular to the scattering plane, Eq. (3), where no Rayleigh angular dependence of scattering occurs, the angular dependence due to particles scattering in the Mie limit after aggregation, which manifests itself in a increased forward scattering, i.e., at  $180^\circ$ .

Figure 1 shows the angular dependence of polarization of 532 nm plasmon-scattered light for a range of gold colloid sizes. The plot starts at a  $40^\circ$  view point, and ends with polarization values at  $300^\circ$  with respect to an excitation angle of  $0^\circ$ . Angles outside these ranges were not measurable due to the physical constraints of the rotational stage and the collection fiber positioning. From Fig. 1 we observe that the plasmon-scatter polarization curves are, as expected, almost symmetrical around the  $180^\circ$  angle, the slight nonsymmetries due to the exact positioning of the excitation beam in the

center of the sample. Of particular interest is the sharp drop in polarization at angles approaching  $180^\circ$ , and also as a function of colloid size.

This interesting observation, which inevitably lends itself to an approach for bioaffinity sensing, can be explained in two ways. First, when a small particle is exposed to an electromagnetic wave whose wavelength is much longer than the diameter of the particle, then every electron in the metallic particle oscillates with the same phase as the wave, and therefore scatters light with the same phase. However, for larger particles when its diameter approaches the wavelength, then electrons in different parts of the particles oscillate with different phases. This leads to interference of the scattered light, sometimes referred to as dephasing,<sup>8,9</sup> where the both the intensity and angular distribution of the scattered light can be significantly different than that of smaller particles. In Fig. 1 at angles close to  $180^\circ$ , we see a decreased polarization for increased colloid size at a given angle, attributed to the dephasing of the scattered light. Second, the magnitude of these polarization changes is manifested in the fact, that greater scattered intensities are observed for an oscillating dipole at angles approaching  $180^\circ$ , i.e., the spatial distribution of scatter increases in the forward direction as a function of size.<sup>8-11</sup> In this regard we have been careful to choose initial unaggregated gold nanoparticles whose diameters are less than  $1/20$ th the wavelength of light, i.e., Rayleigh scatterers,<sup>11</sup> which upon aggregation no longer scatter light in a Rayleigh manner. Rayleigh theory applies quite strictly to particles for which the radius  $a \ll \lambda / (2\pi n_{\text{med}} |m|)$ , where  $n_{\text{med}}$  is the refractive index of surrounding the nanoparticle and  $m$  is the refractive index of the bulk particle itself. For the gold colloids discussed here  $|m|$  is usually not greater than 4.<sup>8,9</sup> Subsequently we can see that for  $|m|=4$ ,  $\lambda=532$  nm and  $n_{\text{med}}=1.33$ , this expression yields ideal Rayleigh scatters of 15.9 nm. According to Yguerabide,<sup>8</sup> particles up to 40 nm diameter can still be considered to be in the Rayleigh limit for visible incident wavelengths.<sup>8</sup>

From Fig. 1 it is also important to note that we see a drop in polarization at angles near  $180^\circ$ , which can be considered to be the angle where one would normally expect a high polarization value due to unaffected incident light, cf. a solution of fluorophores.<sup>12</sup> However, in our system here, the solution optical density was  $\approx 1$ . Subsequently only a very small fraction of the incident light does not interact with the colloids, which are well-known to interact and scatter light outside the constraints of their physical cross sections,<sup>8</sup> when  $Q_{\text{sca}} > 1$ , and where  $Q_{\text{sca}} = C_{\text{sca}} / \pi a^2$ , and  $Q_{\text{sca}}$  is the scattering efficiency,  $a$  is the particle radius, and  $C_{\text{sca}}$  is the scattering cross section.<sup>8</sup>

To demonstrate the utility of our sensing approach and indeed its broader applicability to biological sensing, we choose a model protein system. The streptavidin-biotin system has been widely used for demonstration of nanoscale bioaffinity sensors,<sup>1</sup> primarily due to the extremely high binding affinity,  $K_d \approx 10^{13}$  1/M. Streptavidin is a tetrameric protein, which can bind up to four biotinylated molecules.<sup>1</sup> Subsequently streptavidin can be used to crosslink biotinylated-bovine serum albumin (BSA) coated 20 nm gold colloids, in essence causing the near-field plasmon coupling of the nanoparticles, a subsequent change in their polarization (a function of colloidal proximity) as well as breaking the Rayleigh scattering limit,<sup>8,9</sup> the particles upon



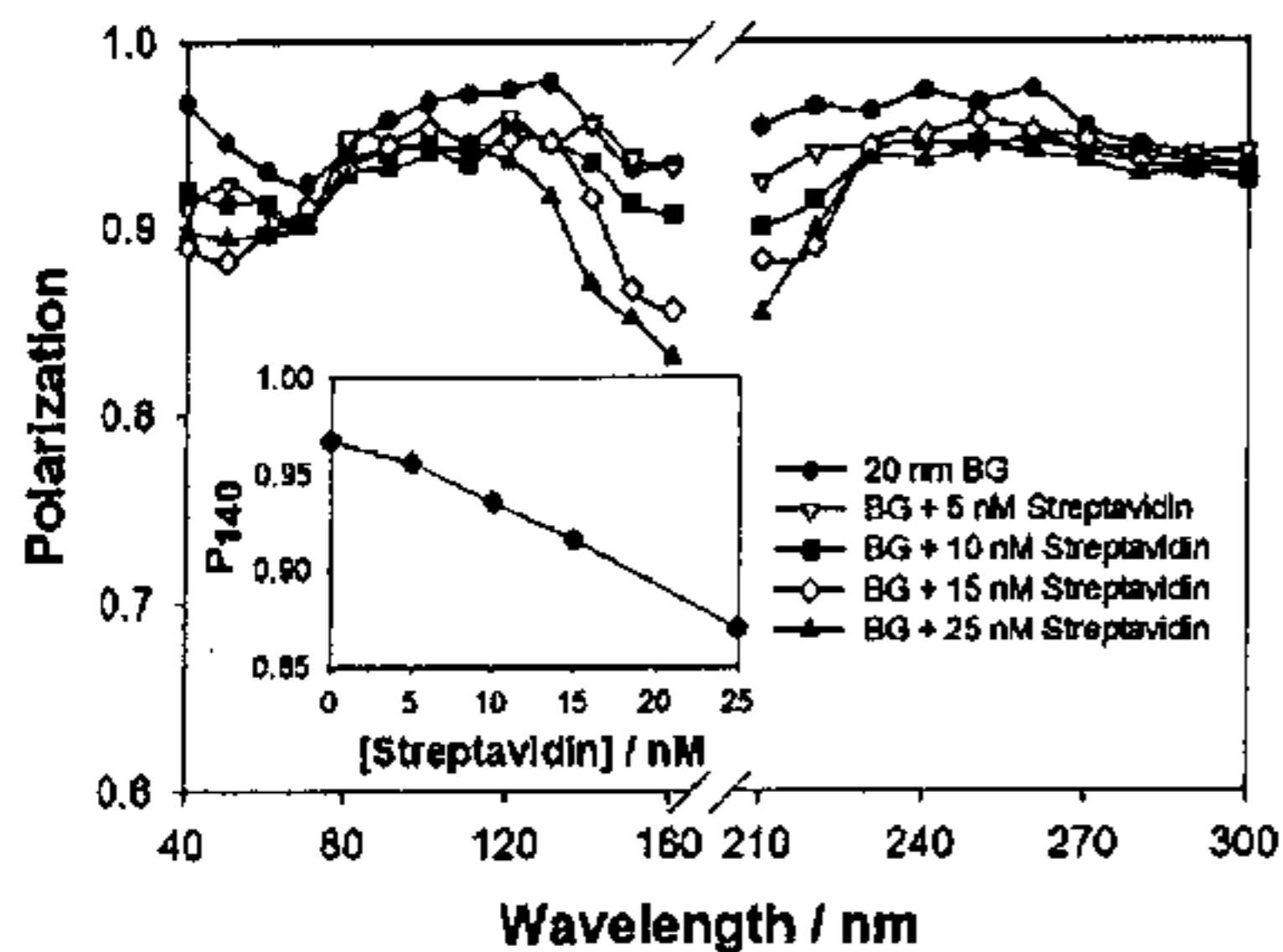


FIG. 2. Angular-dependent polarization of plasmon scatter as a function of nanoparticle aggregation, and the polarization,  $P$ , at 140 deg vs streptavidin concentration (Insert). BG—Biotinylated 20 nm gold colloids.

aggregation starting to scatter in the Mie limit.<sup>8,9</sup> Our initial hypothesis for this effect was based on the results obtained with different sized virgin unaggregated colloids, similar polarization scattering effects being envisaged for increased sized unaggregated colloids, as compared to the aggregation of small colloids.

The surface modification of 20 nm gold colloids was performed using a modified version<sup>7</sup> of the procedure found in the literature.<sup>13</sup> The biotinylated-BSA colloids were used in the aggregation assays with increasing concentrations of streptavidin. In this regard, a 1000 nM stock solution of streptavidin (prepared in polybutene sulfone based on the specifications provided by manufacturer, Sigma/Aldrich,  $E1\%$  at 282 nm=31.0) was added to 0.5 mL of biotinylated gold colloid samples and incubated at room temperature for 30 min. In order to achieve the desired final streptavidin concentrations, predetermined volumes of streptavidin stock solution were used. The angle-dependent polarized scattering from gold colloids of various sizes and those used in the aggregation assay were measured using an X-Y rotating stage (Edmund Optics), that was modified to hold a cylindrical cuvette (a thin walled glass NMR tube), with a fiber optic mount. The gold colloids were illuminated with a 532 nm laser line, a neutral density filter being used to adjust the laser intensity. The angle-dependent polarized scattered light from the gold colloids was collected through a dichroic sheet polarizer (Edmund optics) into a 600 micron broad wavelength fiber that was connected to an Ocean Optics HD2000 spectrofluorometer.

Similar to the polarization measurements of the virgin colloids as a function of colloidal size, the 20 nm biotinylated-BSA coated gold particles showed a substantial decrease in polarization at an angle approaching 180° upon increasing additions of streptavidin, Fig. 2—top. This decrease is explained as due to the near-field coupling of surface plasmons upon aggregation,<sup>1,2</sup> which results in dephased polarized scatter<sup>1,2,8,9</sup> similar to the effect observed for increasing colloid size, i.e., Fig. 1. As the concentration of streptavidin in the sample increases we also observe an increase in the width of the scatter band at 180°, i.e., an in-

crease in the extent of forward scatter as the aggregated particles no longer scatter within the Rayleigh limit,<sup>8,9</sup> but indeed now begin to scatter light as described by Mie theory.<sup>10</sup> Subsequently the concentration of streptavidin can be readily determined, Fig. 2—insert, as could any other biospecies which induces particle flocculation.

In conclusion, we report our findings of polarized angular-dependent affinity biosensing for solutions of nanoparticles. This model sensing platform could be potentially applied to many other nanoparticle assays.<sup>1,2</sup> Interestingly, fluorescence depolarization is widely used in high throughput screening (HTS) and drug discovery.<sup>12,14</sup> In HTS assay plate-well formats, minute changes in fluorescence polarization are readily used to determine antigen binding, reflecting a change in the mobility of a fluorophore. Our approach suggests that polarization based assays can be performed with a simple near-180° geometry detection of the scattered light, as compared to the total-internal reflection fluorescence<sup>12,14</sup> or backscattered fluorescence geometries currently employed.<sup>12,14</sup> Further, in our approach, an assay “hit” could be determined by colloid proximity and not rotational orientation as is currently used to transduce polarization assays.<sup>12</sup> In addition, the nanoparticles are inherently more photostable than fluorophores, do not settle out solution, and can couple over 2.5 times their diameter,<sup>3</sup> enabling long-range plasmon coupling and therefore the sensing of large antigens. In this regard, fluorescence resonance energy transfer has languished for long-range immunoassay measurements, due to the short-range fluorophore Forster-type coupling distances, typically <5 nm.<sup>12</sup> Work is currently underway by our laboratories in this regard and will be reported in due course.

This work was supported by the NIH, National Center for Research Resources, RR008119. Partial salary support to C.D.G. and J.R.L. from the University of Maryland Biotechnology Institute is also acknowledged.

<sup>1</sup>D. A. Stuart, A. J. Haes, C. R. Yonzon, E. M. Hicks, and R. P. Van Duyne, *IEE. Proc.-Nanobiotechnol.* **152**, 13 (2005).

<sup>2</sup>E. Hutter and J. H. Fendler, *Adv. Mater. (Weinheim, Ger.)* **16**, 1685 (2004).

<sup>3</sup>K.-H. Su, Q.-H. Wei, X. Zhang, J. J. Mock, D. R. Smith, and S. Schultz, *Nano Lett.* **3**, 1087 (2003).

<sup>4</sup>S. Schultz, D. R. Smith, J. J. Mock, and D. A. Schultz, *Proc. Natl. Acad. Sci. U.S.A.* **97**, 996 (2000).

<sup>5</sup>J. J. Mock, D. R. Smith, and S. Schultz, *Nano Lett.* **3**, 485 (2003).

<sup>6</sup>K. Aslan, J. R. Lakowicz, and C. D. Geddes, *Anal. Chem.* **77**, 2007 (2005).

<sup>7</sup>K. Aslan, P. Holley, L. Davies, J. R. Lakowicz, and C. D. Geddes, *J. Am. Chem. Soc.* **127**, 12115 (2005).

<sup>8</sup>J. Yguerabide and E. Yguerabide, *Anal. Biochem.* **262**, 137 (1998).

<sup>9</sup>J. Yguerabide and E. Yguerabide, *Anal. Biochem.* **262**, 157 (1998).

<sup>10</sup>G. Mie, *Ann. Phys.* **25**, 377 (1908).

<sup>11</sup>M. Kerker, *The Scattering of Light and Other Electromagnetic Radiation* (Academic, New York, 1969).

<sup>12</sup>J. R. Lakowicz, *Principles of Fluorescence Spectroscopy* (Kluwer/Academic Plenum, New York, 1997).

<sup>13</sup>R. A. Reynolds, C. A. Mirkin, and R. L. Letsinger, *J. Am. Chem. Soc.* **122**, 3795 (2000).

<sup>14</sup>*Drug Discovery Handbook*, edited by Shayne Gad (Wiley, New York, 2005).